Quantum chemical dissection of the classic terpinyl/pinyl/bornyl/camphyl cation conundrum—the role of pyrophosphate in manipulating pathways to monoterpenes†‡

Young J. Hong and Dean J. Tantillo*

Received 24th May 2010, Accepted 13th July 2010
DOI: 10.1039/c0ob00167h

Based on quantum chemical studies, mechanisms to form bornyl diphosphate from geranyl diphosphate are suggested. While bornyl diphosphate is usually proposed to be generated *via* combination of the pyrophosphate group with a secondary bornyl cation, quantum chemical computations indicate that the bornyl cation is actually not a minimum. Instead, concerted attack of the pyrophosphate group coupled with an alkyl shift could yield bornyl diphosphate from either the pinyl cation or the camphyl cation. Hints of bifurcating pathways on the energy surfaces for such reactions were also uncovered. Of particular note is the development and validation of a large model of the pyrophosphate counterion treated entirely with quantum chemistry.

Introduction

Among the many varieties of natural products known, terpenes (and derived terpenoids) perhaps display the most diverse and complex carbon skeletons. Terpenoid natural products exhibit a wide range of biological activities and play many vital ecological roles. For instance, monoterpenes are major constituents of the oleoresin secreted at sites of damage to conifers.[1] Many monoterpenes also have physical properties that form the basis for using certain plants in fragrance, culinary flavoring and medicinal applications.[2,3]

Monoterpenes are derived from geranyl diphosphate (GPP; **1**, Scheme 1) through multistep rearrangement/cyclization reactions of carbocations that are generated upon dissociation of the pyrophosphate group.[2,3] This moiety, however, along with associated magnesium ions and water molecules, resides close to the carbocations generated in terpene synthase active sites during monoterpene production. Although various roles for enzyme-bound pyrophosphate have been proposed (*e.g.*, providing electrostatic stabilization of cationic intermediates and transition state structures, serving as the base that deprotonates a carbocation to form alkene products), evidence for the specific role(s) of pyrophosphate during terpene-forming reactions remains circumstantial.[4,5] Herein, we disclose results of quantum chemical calculations that provide atomic-resolution pictures of energetically viable chemical events in monoterpene-forming reactions in which the role of nearby pyrophosphate is apparent. Although these results also constitute circumstantial evidence, we hope that the detailed pictures of pyrophosphate reactivity that we provide will prove useful in focusing the design of future experiments.

Department of Chemistry, University of California, Davis, One Shields Avenue, Davis, CA, 95616. E-mail: tantillo@chem.ucdavis.edu

† This paper is part of an *Organic & Biomolecular Chemistry* web theme issue on chemical biology.

‡ Electronic supplementary information (ESI) available: Coordinates and energies for all computed structures and additional details on computations not discussed at length in the text. See DOI: 10.1039/c0ob00167h

Previously, we have used quantum chemical methods to study carbocation rearrangements leading to a wide variety of complex terpene natural products—both sesquiterpenes[6–11] and diterpenes.[12–14] The work described herein extends our efforts in unraveling fundamental mechanistic principles that govern the course of terpene-forming reactions, both in the absence and presence of components of terpene synthase enzymes, to the monoterpene realm. The nature of the connections between various GPP-derived carbocations (Scheme 1) has been pondered and debated for decades;[3,15,16] we hope the results of our computations will help clarify this complex reaction network.

Bornyl diphosphate synthase (BPPS),[17–19] which mediates the transformation of GPP (**1**, Scheme 1) to bornyl diphosphate (BPP; **4**, Scheme 1), is unusual in that this enzyme incorporates a pyrophosphate group in its final product, whereas terpene synthase reactions are generally terminated by deprotonation to form alkenes or water-trapping to form alcohols. The BPPS-mediated reaction thus offers an excellent system for which to investigate not only the potential role of pyrophosphate in providing noncovalent stabilization of carbocations, or as a base, but also as a nucleophile.

The primary focus of our study was on assessing the viability of possible reaction mechanisms for the production of bornyl diphosphate (BPP, **4**), α/β-pinene (**2–3**) and α/β-camphene (**5–6**). A second aim, however, was to use this system to provide evidence for the validity of various computational methods in modeling terpene-forming carbocation rearrangements in general. Although we typically use the mPW1PW91/6-31+G(d,p)//B3LYP/6-31+G(d,p) method for computing carbocation reaction pathways,[6–14] we have previously compared results obtained at this level of theory with those obtained using other selected methods.[13,20,21] Herein we describe a broader survey of theoretical methods, highlighting their performance in terms of computing both geometries and energies.

Our third aim was to introduce theoretical models of enzyme-bound pyrophosphate for use in future modeling work. In our previous studies, effects of electron-rich groups on carbocations were examined using simple models such as ammonia and

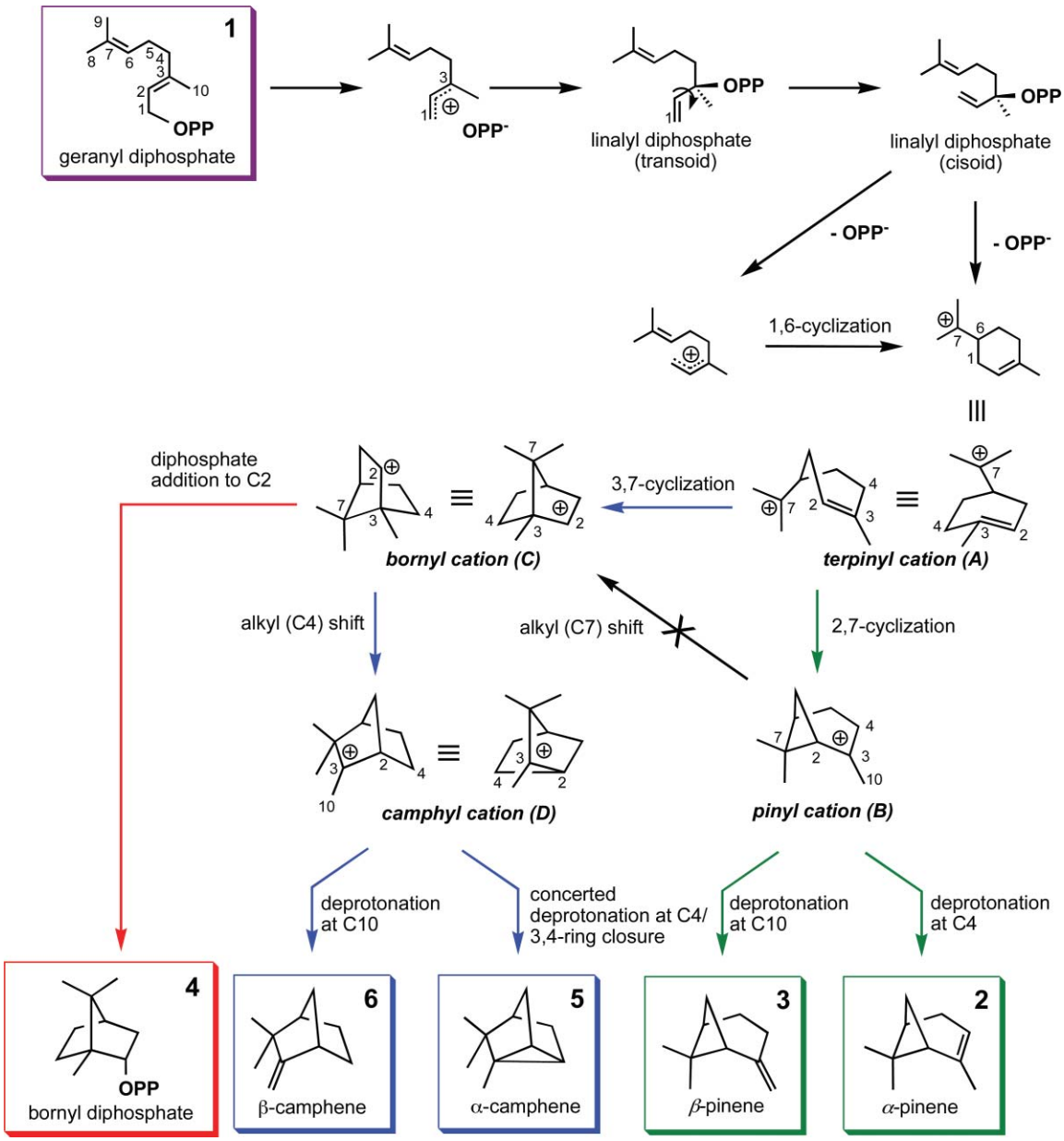

Scheme 1

water.[6,10,14,21,22] In the present work, we extend this approach to include the pyrophosphate group, surveying several possible models of this group—many of which are larger than the carbocations with which they interact—and providing recommendations for future modeling.

During the completion of this study and preparation of this manuscript, an excellent theoretical study on the BPPS reaction was reported by Weitman and Major.[23] In this work, a variety of theoretical methods were surveyed (some the same as those we examined, some different) for their performance in computing geometries and energies of small carbocations (containing up to four carbons). Our comparison of various methods for treating full-sized GPP-derived carbocations (*vide infra*) led to a similar, but slightly different, assessment of the validity of commonly used and readily accessible methods. The study of Weitman and Major also provided a detailed picture of the energy surface for a variety of rearrangements of GPP-derived carbocations in the absence of an enzyme. Our results (obtained using different theoretical methods) corroborate theirs. Importantly, Weitman and Major also described the first (to our knowledge) theoretical treatment of a terpene synthase reaction where pyrophosphate was treated with quantum mechanics. This was accomplished *via* molecular dynamics simulations, utilizing a quantum mechanics/molecular mechanics (QM/MM) approach, on BPP formation using an intact BPPS. Our studies complement this work by providing additional insights into the role of pyrophosphate in the formation of BPP and other monoterpenes and by demonstrating that many key features of the enzymatic reaction can be captured through the use of well-chosen small (compared to the size of the whole enzyme) models.

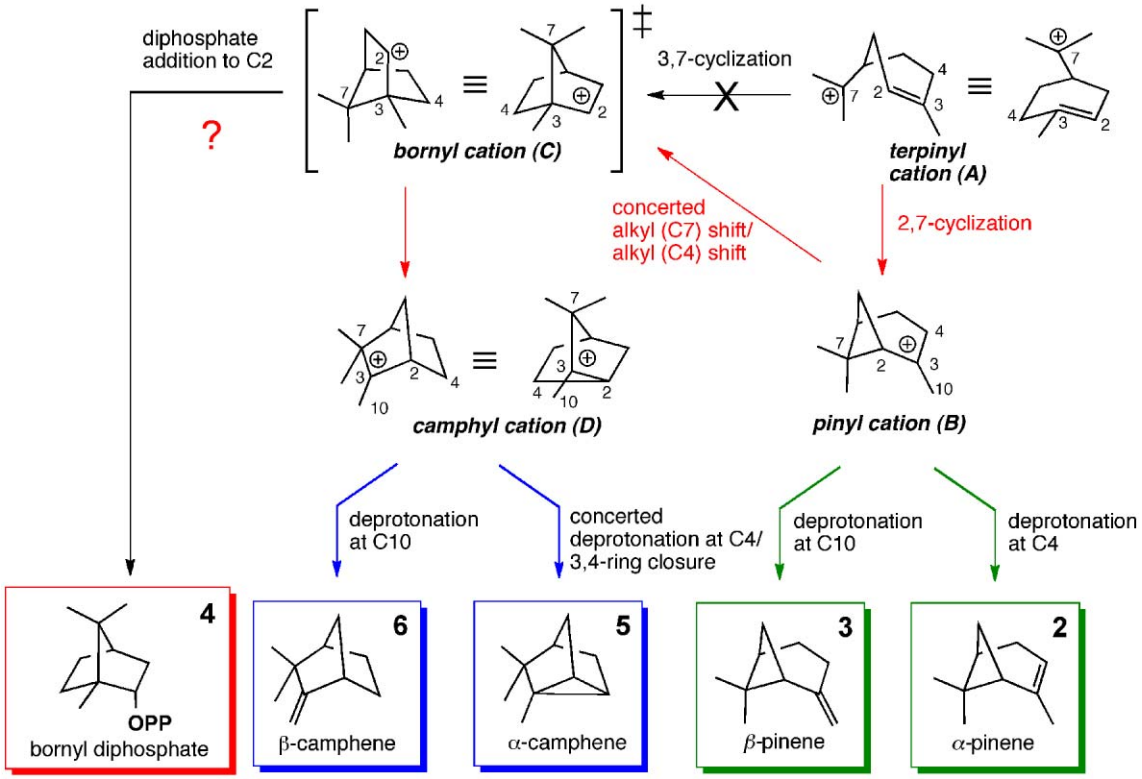

Scheme 2

Methods

All calculations were performed with GAUSSIAN03.[24] All geometries for the uncomplexed system were optimized using the B3LYP method.[25] Our previous studies have suggested that the B3LYP method performs reasonably well in predicting geometries and reactivity of carbocations.[6–14,21,22,26,27] Recent reports indicate that mPW1PW91, PBE, mPWB1K and BB1K also perform well for carbocation structures and reactions.[23,28,29] To further assess the performance of the B3LYP method for terpene-forming carbocation rearrangements, we performed comparisons with the mPW1PW91,[30] PBE,[31] mPWB1K,[32] BB1K[33] and MP2[34] methods (see below and Supporting Information‡ for additional details). We have used some of these methods previously in the studies of other terpene-forming carbocation rearrangement reactions, in particular mPW1PW91 single-point energies.[6–14,27] All stationary points were characterized by frequency calculations and reported energies include zero-point energy corrections (unscaled) from the method used for geometry optimization. All reported calculations involving the diphosphate group were performed at the B3LYP/6-31G(d) level of theory, although, for comparison, B3LYP/6-31+G(d,p) calculations were performed for selected systems (see Supporting Information‡ for details). Intrinsic reaction coordinate (IRC) calculations were used for further characterization of all transition state structures,[35] and IRC plots for all transition state structures are shown in the text or in the Supporting Information.‡ Structural drawings were produced using *Ball & Stick*.[36] Atom numbering indicated in the structures in this report is based on that of GPP (**1**, Scheme 1). For simplicity, all computed structures shown below have absolute configurations based on the (*R*)-terpinyl cation.

Results and discussion

Rearrangement of the terpinyl cation (A)

The previously proposed mechanisms for the conversion of GPP to the monoterpenes of interest (**2–6**) are generally very similar to those shown in Scheme 1.[15,17,18] The terpinyl cation (**A**) is proposed to be a key intermediate from which the reaction branches into two pathways, one leading to the pinyl cation (**B**) and the other leading to the bornyl cation (**C**). The pinyl cation could be a direct precursor to both α-pinene (**2**) and β-pinene (**3**), while the bornyl cation could be a direct precursor to BPP (**4**). Rearrangement of the pinyl cation to the bornyl cation *via* a 1,2-alkyl shift could also occur, although this possibility was previously discounted (for the pinene cyclases) based on interpretations of the results of kinetic isotope effect experiments.[15] Rearrangement of the bornyl cation to the camphyl cation (**D**) could lead to α-camphene (**5**) and β-camphene (**6**).

Using the B3LYP/6-31+G(d,p) method, intermediates **A**, **B** and **D**, and transition state structures connecting **A** to **B** and **B** to **D** were located. Carbocation **C** was not found as a minimum in the gas phase, although the **B**-to-**D** transition state structure resembles this species. A revised reaction network taking these results into account is shown in Scheme 2 and computed geometries and energies for the structures involved are shown in Fig. 1. Similar conclusions were reached by Weitman and Major based on BB1K/6-31+G(d,p) calculations,[23] and our results using other levels of theory (*vide infra*) also provide similar pictures of this energy surface.

The first expected reaction after the formation of the terpinyl cation (**A**) involves cation-alkene cyclization. Attack of the

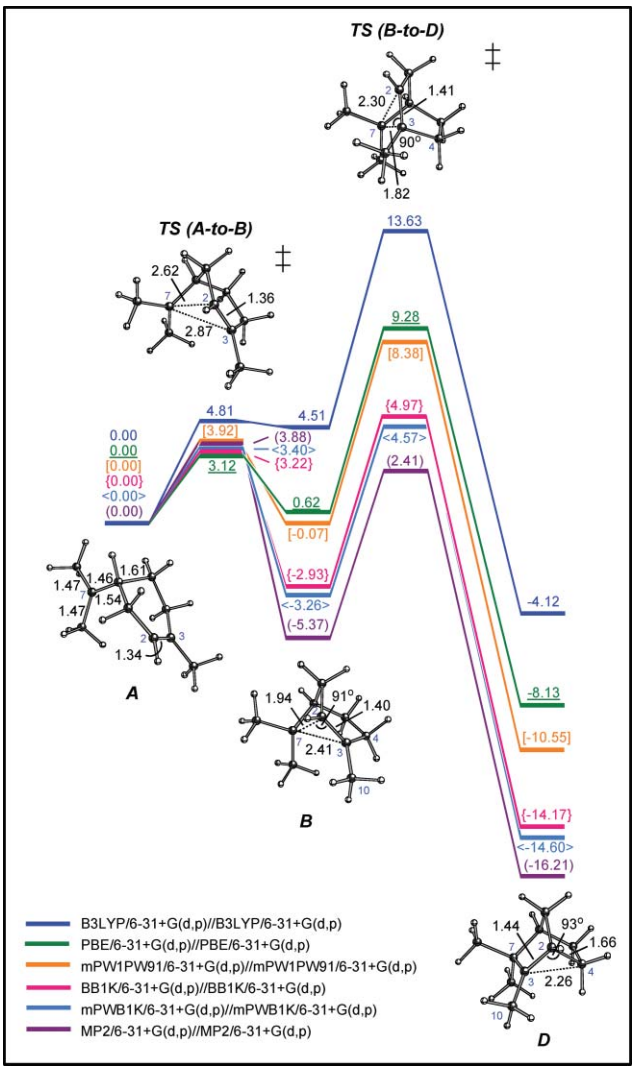

Fig. 1 Reaction profile for rearrangement of the terpinyl cation (**A**). Computed geometries (selected distances in Å; for B3LYP) and energies (kcal mol^{-1}, relative to the energy of **A**; for all levels of theory shown based on fully optimized structures at that level; see Supporting Information‡ for geometries) of minima and transition state structures are shown.

C2═C3 π-bond on C7 is expected to convert the terpinyl cation to either the pinyl cation (**B**) *via* 2,7-cyclization or the bornyl cation (**C**) *via* 3,7-cyclization (Scheme 1). The transition state structure that looked as expected for 2,7-cyclization of the terpinyl cation was indeed found to connect **A** with **B** (Fig. 1). The conversion of **A** to **B** has a computed barrier of approximately 5 kcal mol^{-1} using the B3LYP/6-31+G(d,p) method and this method predicts that the cyclization is an endothermic process. Note that the C2–C7 distance in the computed structure of **B** (1.94 Å) is quite long. Nevertheless, it is reasonable to consider this structure to be a pinyl cation with its newly formed C2–C7 σ-bond elongated due to strong hyperconjugation with the formal cation at C3 and the strain associated with a 4-membered ring.[6,7,37,38] Alternatively, **B** may be formulated as another form of **A** with a very tight intramolecular cation-π interaction.[6,7,11,21,38,39] The difference in the C2–C7 and C3–C7 distances reflects, at least in part, the different degrees of substitution of the two carbons of the formal π-bond.

The geometry of intermediate **B** was also computed using the mPW1PW91, PBE, mPWB1K, BB1K and MP2 methods, all with the 6-31+G(d,p) basis set. In general, similar geometries were obtained, although some differences were observed. For example, the C7–C2–C3 angle varies from 84° to 93°, being smallest in the MP2 structure and largest in the PBE structure, and the C2–C7 distance ranges from 1.77 to 1.94 Å, being shortest in the mPWB1K structure and longest in the B3LYP structure. Not surprisingly, the MP2 method predicts a structure that is significantly more bridged (*i.e.*, more nonclassical) than do the density functional methods (see Supporting Information‡ for additional details).[22,26,40]

The predicted barrier for the conversion of **A**-to-**B** does not vary much with the level of theory used, ranging from 3.12 kcal mol^{-1} with the PBE method to 4.81 kcal mol^{-1} with the B3LYP method (Fig. 1). The predicted energy of **B**, relative to that of **A**, does vary significantly, however, ranging from +4.51 kcal mol^{-1} with B3LYP to approximately zero with both the PBE method and mPW1PW91 methods, down to −5.37 with the MP2 method (Fig. 1). The well-known tendency of the B3LYP method to underestimate the energies of cyclic structures compared to acyclic structures is again observed here,[29] as is the well-known tendency of the MP2 method to favor bridged carbocation structures.[22,26,40] At none of the levels of theory examined was a classical pinyl cation (*i.e.*, with a short C2–C7 bond) found as a minimum.

We also examined the susceptibility of the geometry of **B** to changes induced by intermolecular interactions with electron rich groups. The C2–C7 distance can indeed be decreased significantly upon C–H···X interaction,[6,10,21,22,38] dropping to 1.77 Å and 1.59 Å (B3LYP) upon complexation with ammonia at C4–H_{exo} and C4–H_{endo}, respectively.[41] These examples hint that the structure of **B** may be modulated significantly by the surrounding active site of a monoterpene synthase, perhaps by interaction with the departed pyrophosphate group (*vide infra*).

As mentioned above, we were unable to locate a gas phase minimum corresponding to the bornyl cation. Instead, the transition state structure connecting **B** directly to **D** resembles a highly hyperconjugated bornyl cation (Scheme 2 and Fig. 1 and 2). Formation of **D** from **B** is predicted to be a concerted process with two alkyl-shifting events occurring asynchronously[38,42] (C7 migration from C2 to C3, and C4 migration from C3 to C2, Fig. 2)—a formal

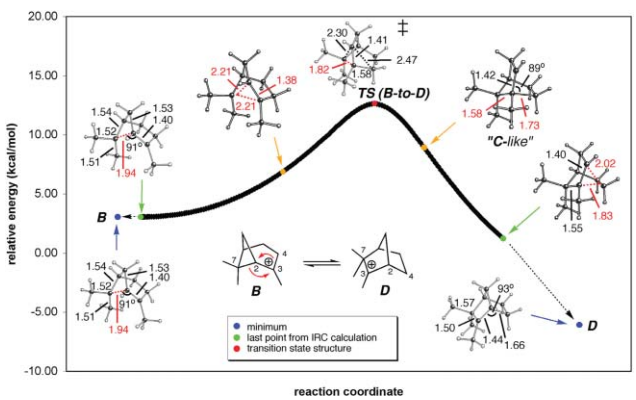

Fig. 2 Conversion of **B** to **D** from IRC calculations (B3LYP/6-31+G(d,p); energies do not include zero-point energy corrections).

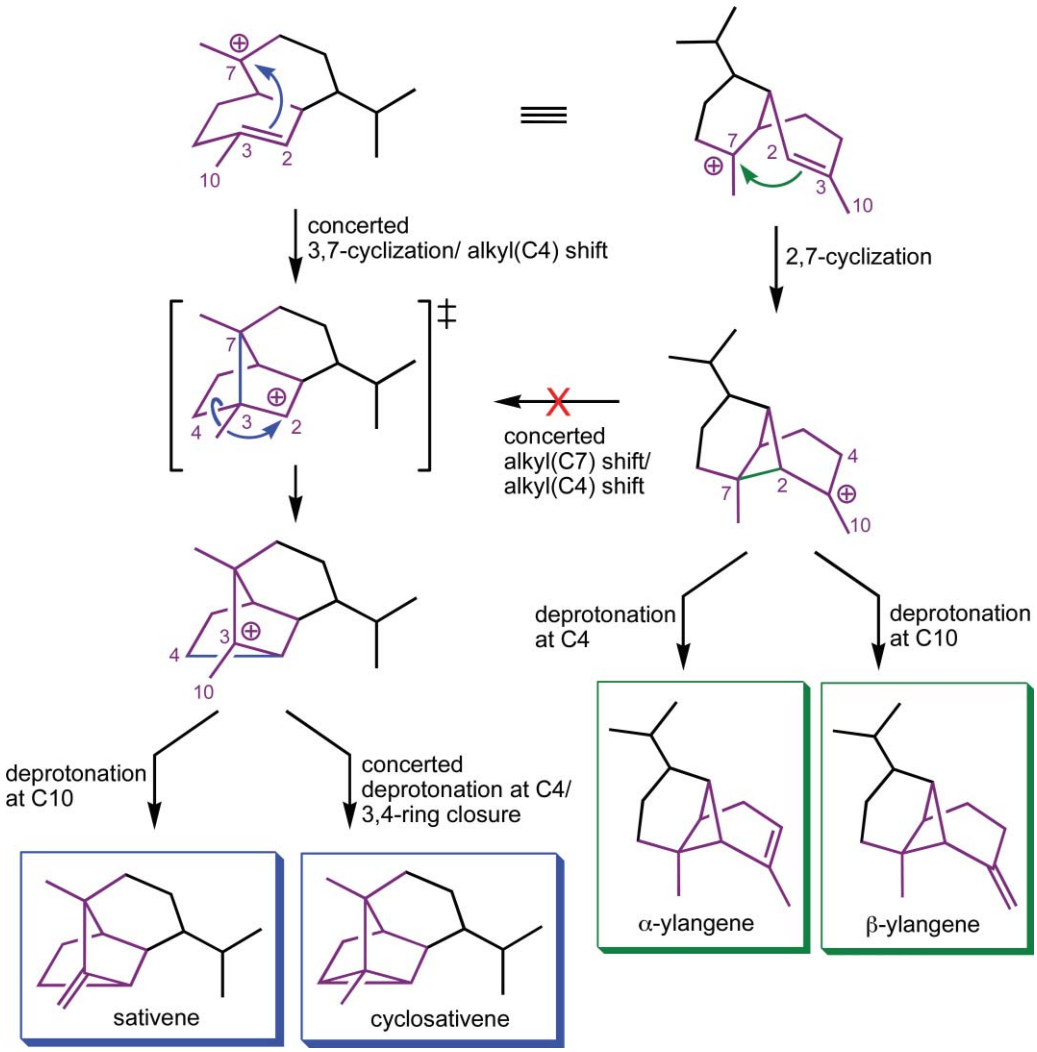

Scheme 3

dyotropic rearrangement.[42,43] Concerted reactions of this sort, that avoid the formation of secondary carbocations, have been predicted previously for a variety of other terpene forming carbocationic rearrangements.[6,10,14,29,38,42,44] For example, closely related rearrangements have been described in a recent computational study on formation of the sesquiterpenes cyclosativene, sativene, α-ylangene and β-ylangene.[6] The reactions leading to α-pinene and β-pinene (Scheme 2) are directly analogous to those that form α-ylangene and β-ylangene (Scheme 3, right; the portion of the sesquiterpene skeleton that corresponds to the monoterpene system is highlighted). However, the reactions that lead to α-camphene and β-camphene are not directly analogous to the reaction that forms sativene, since formation of the carbocation that precedes sativene involves concerted ring closure and alkyl shift (Scheme 3; left) instead of dyotropic rearrangement (*i.e.*, the sativene-forming pathway would be analogous to a direct **A**-to-**D** pathway). A similar situation was encountered in our studies on the formation of the zizaenes and related sesquiterpenes; transition state structures with closely related, secondary cation-like, geometries were found to occur along reaction coordinates corresponding to significantly different asynchronous combinations of events, *i.e.*, transition state structures for ring-closure/alkyl shift closely resembled those for dyotropic rearrangement.[10,45] In short, it is far from straightforward to predict which minima are connected to secondary cation-like transition state structures just based on their geometries.[46]

The C3–C7 distance in the **B**-to-**D** transition state structure also varies somewhat depending on the level of theory used, ranging from 1.72 to 1.85 Å, being shortest in the mPWB1K structure and longest in the PBE structure (see Supporting Information‡ for details), while the C7–C3–C2 angle varies only slightly (88°–91°). The C2–C4 distance in structure **D** varies from 1.64 to 1.72 Å, being shortest in both the mPW1PW91 and mPWB1K structures and longest in the MP2 structure, while the C3–C2–C4 angle ranges from 81° to 93°, being smallest in the MP2 structure and largest in the B3LYP structure (see Supporting Information‡ for details).[48] The barrier for the **B**-to-**D** rearrangement step is predicted to be relatively insensitive to the computational method used, however, ranging from 7.78 to 9.12 kcal mol^{-1} from **B**. The exothermicity of this step varies from 8.63 to 11.34 kcal mol^{-1} (Fig. 1). All of the methods examined, except the MP2 method, predict that the transition state structure for the **B**-to-**D** rearrangement will be higher in energy than the transition state structure for the **A**-to-**B** step.

In that most of our previous work on carbocation rearrangements has made use of B3LYP geometries (generally coupled to mPW1PW91 single point energies),[6–14] we computed single point energies on the B3LYP geometries shown in Fig. 1, using the levels of theory at which we had already recalculated geometries (Fig. 1), to see if using B3LYP geometries is indeed a reasonable approach. Interestingly, despite the method-dependent changes to geometries discussed above, the computed energetics for the **A**-to-**B**-to-**D** reaction sequence from single point calculations closely mirror those calculated with fully reoptimized geometries (compare Fig. 1 with Fig. 3), suggesting that at least in this case (and perhaps in many others involving carbocation rearrangements), the use of B3LYP geometries is quite reasonable (we use these throughout the remainder of the manuscript), and also that the potential energy surfaces around each stationary point are rather flat with respect to the geometric variations described above.

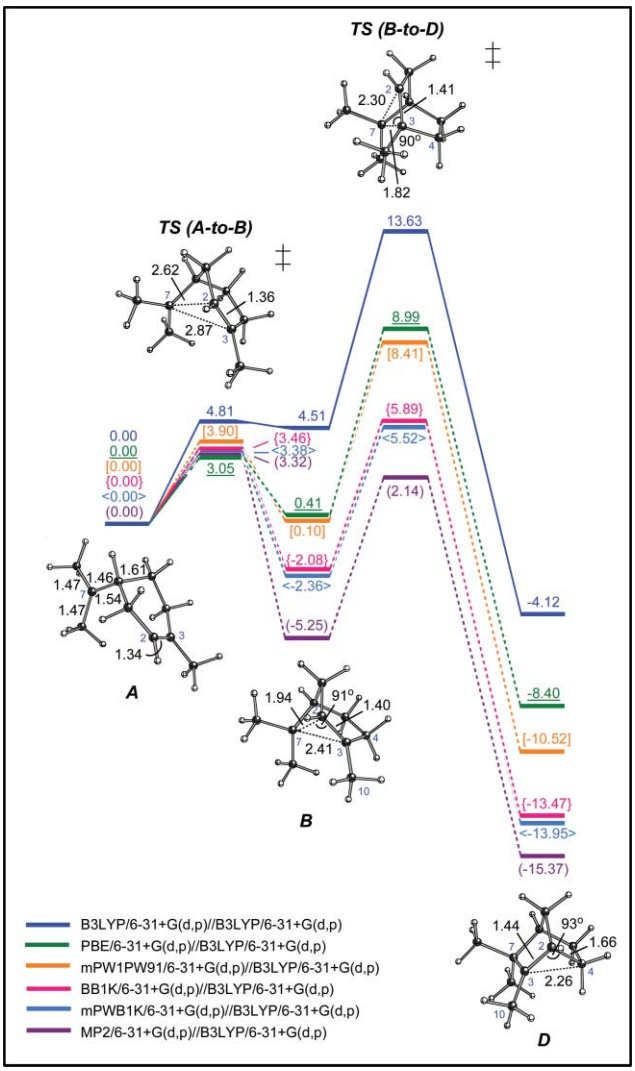

Fig. 3 Reaction profile for rearrangement of the terpinyl cation **A**. Computed geometries (selected distances in Å; B3LYP/6-31+G(d,p)) and energies (kcal mol^{-1}, relative to the energy of **A**) of intermediates and transition structures are shown. Energies include zero point energy corrections from frequency calculations using B3LYP/6-31+G(d,p).

Given that our calculated energy surfaces imply that the connections between cations **A–D** should be modified from the picture in Scheme 1, so must some of the steps that lead to the ultimate monoterpene products. As in previously proposed reaction schemes (*e.g.*, Scheme 1), we propose that direct deprotonation at C4 or C10 of **B** should lead to α-pinene (**2**) or β-pinene (**3**), respectively, direct deprotonation at C10 of **D** should generate β-camphene (**6**) and concerted deprotonation/ring closure should generate α-camphene (**5**, Schemes 1 and 2). However, in our proposed reaction pathway (Scheme 2 and Fig. 1), it is unclear which cation will be the direct precursor to BPP (**4**), since we predict that the bornyl cation (**C**) is not a minimum; this issue is addressed below.

Formation of bornyl diphosphate

BPP could, in principle, be formed from the secondary bornyl cation (**C**) *via* direct nucleophilic addition of pyrophosphate to C2 (Scheme 1), but, as mentioned above, **C** appears not to be a minimum (at least in the absence of an enzyme). Alternatively, concerted alkyl shift/pyrophosphate addition to C2 of either the pinyl (**B**) or camphyl (**D**) cation could yield BPP. Similar processes have been predicted for the formation of related terpenols.[10,14] In that we have, on occasion, found secondary cation minima when such structures are complexed to lone pair donors like ammonia or water,[10,14,42] it seemed possible that cation **C** might be an intermediate in the presence of the enzyme, but we were unable to locate any such complexes for cation **C** using the lone pair donors described below; consequently, we favor mechanisms that do not involve discrete bornyl cation minima even in the active sites of terpene synthase enzymes.

Ammonia as a model nucleophile. We have previously used ammonia as a simple lone pair donor in examining the deprotonation of a variety of carbocations to yield olefinic sesquiterpene products.[6,10,14] Consequently, we began our studies on nucleophilic addition to GPP-derived carbocations using ammonia as a nucleophile. Although ammonia is quite different than enzyme-bound pyrophosphate, it allows us to examine the reactivity of the carbocations in question with a small, symmetrical nucleophile (one could argue that this behavior corresponds to their "inherent" electrophilic reactivity), which can then be compared with the reactivity in the presence of larger, more complex nucleophiles. Using ammonia also allows us to compare our results with previous results on deprotonation.

We located a transition state structure that initially appeared, based on its geometry, to connect either the terpinyl and pinyl cations or the pinyl and camphyl cations in the presence of ammonia (**TS1**, Fig. 4, top). IRC calculations indicated that this structure actually connects an ion-molecule complex of the pinyl cation (**B**·NH_3) to bornylammonium (**7**-H^+, Fig. 4 and Scheme 4). In the **B**·NH_3 complex, the ammonia interacts with both C4–H_{exo} and C10–H *via* weak C–H $\cdots$ N interactions,[21,22] which situate the ammonia above the cationic center (C3---N distance of 3.09 Å and C2---N distance of 3.44 Å). In the transition state structure, the distance between C2 and the nitrogen of ammonia is 2.63 Å, while the C2–C7 distance is increased to 2.16 Å and the C3–C7 distance is reduced to 2.09 Å, consistent with attack on C2 being coupled to a shift of C7 to C3. Note also that in the transition state structure, the forming C2–N bond is *anti* to the lengthening

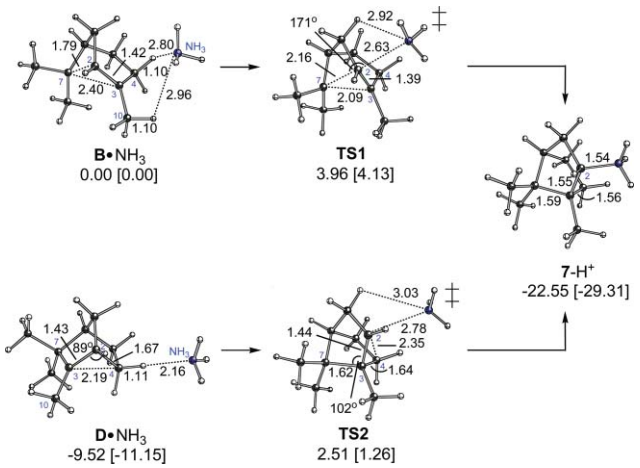

Fig. 4 Ammonia-**B** and ammonia-**D** complexes, transition state structures for ammonia attack and ammonia addition product (**7**-H$^+$). Selected distances (Å) and energies (kcal mol^{-1}; relative to the energy of the **B**·NH$_3$ complex; B3LYP/6-31+G(d,p)//B3LYP/6-31+G(d,p) in normal text and mPW1PW91/6-31+G(d,p)//B3LYP/6-31+G(d,p) in brackets) are shown.

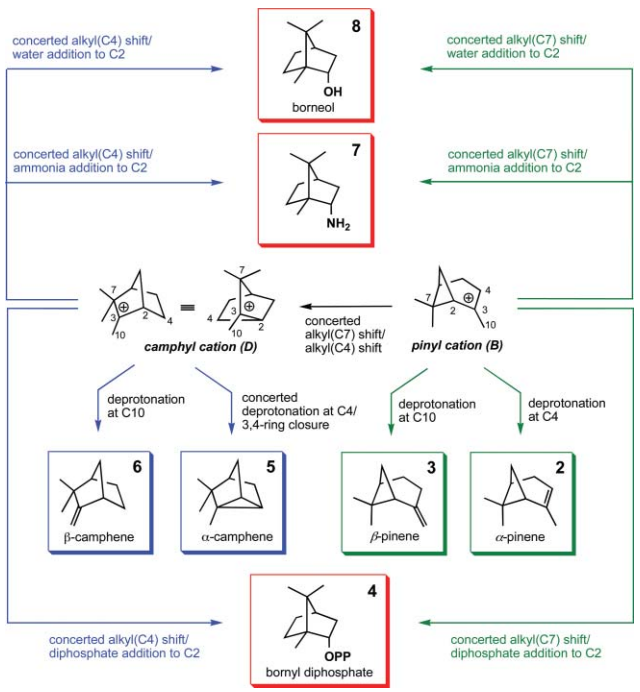

Scheme 4

C2–C7 bond; *i.e.*, the N---C2---C7 substructure resembles the core of a transition state structure for an S_N2 reaction. IRC calculations also provide convincing evidence that attack of ammonia at C2 of **B** is accompanied by the shift of C7 to C3 (Fig. 5a).[49]

We also located another transition state structure that resembles a transition state structure for ammonia addition to C2 of the hypothetical bornyl cation (**TS2**, Fig. 4, bottom). However, IRC calculations indicated that this transition state structure actually connects a camphyl cation-ammonia complex (**D**·NH$_3$, which again sports a C–H···N interaction) to **7**-H$^+$ (Fig. 5b). Our

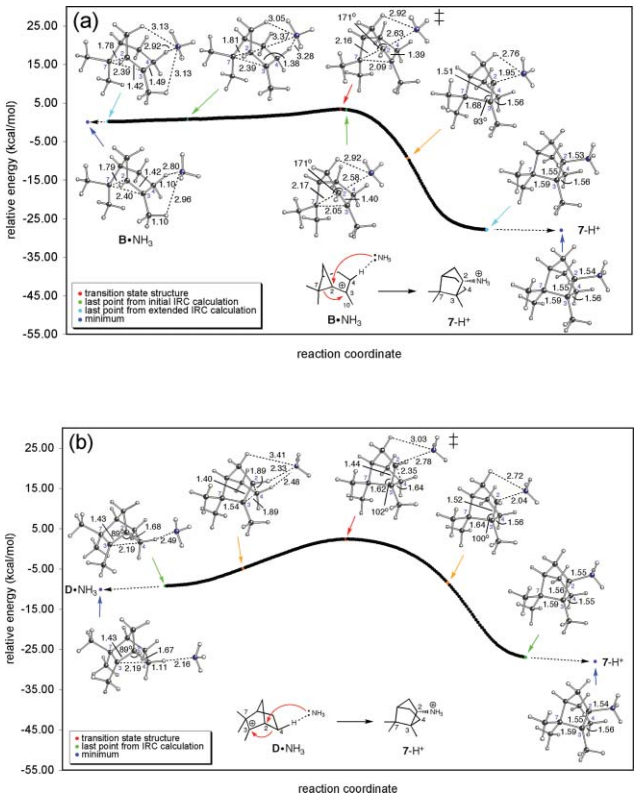

Fig. 5 Conversion of (a) **B**·NH$_3$ and (b) **D**·NH$_3$ to **7**-H$^+$ from IRC calculations (B3LYP/6-31+G(d,p); energies in kcal mol^{-1} relative to the energy of **B**·NH$_3$). The initial IRC calculations toward the **B**·NH$_3$ complex (run using "calcfc") and **7**-H$^+$ in part (a) stopped at the points indicated in green (geometries shown); additional extended IRC calculations were then carried out, each using the wavefunction, geometry and force constants from the last point of the previous IRC calculations (*i.e.*, using "rcfc").

IRC calculations indicate that, although concerted, the alkyl shift largely precedes attack of ammonia, which here occurs *syn* to the breaking C2–C4 bond, thereby leading to transient geometries resembling the hypothetical bornyl cation (Fig. 5b, righthand side).

Interestingly, geometries encountered along the IRC path from **TS1** toward **7**-H$^+$ (Fig. 5a, righthand side) resemble **TS2** (Fig. 4 and 5b). This hints that the pathways from **B**·NH$_3$ and **D**·NH$_3$ may converge en route to **7**-H$^+$. If this convergence were to occur near to **TS2**, this situation could also be viewed as the pathway from **B**·NH$_3$ bifurcating in the **TS2** region between **D**·NH$_3$ and **7**-H$^+$.[13,22,43a,47] This also hints that **B**-to-**D** rearrangement in an enzyme may be difficult to separate from adduct formation (*vide infra*).[50]

Water as a model nucleophile. Our calculations using water instead of ammonia (reactions that would ultimately produce borneol (**8**), Scheme 4), led to qualitatively similar results. Transition state structures similar to **TS1** and **TS2** of Fig. 4 were located and IRC calculations again suggested that the pathway from **B** may bifurcate (here between protonated borneol and a water complex of **D**). Detailed descriptions of these energy surfaces can be found in the Supporting Information.‡

Pyrophosphate models. Do the peculiarities of the pathways leading to apparent bornyl cation adducts persist when more realistic models of enzyme-bound pyrophosphate are used? Finding a chemically meaningful and computationally well-behaved model of bound pyrophosphate proved to be a difficult task. A variety of potential models were examined (Fig. 6a). Although most were fraught with pitfalls (see Supporting Information‡ for details), we ultimately settled on the monoanionic model shown in Fig. 6b (which would lead to an overall neutral system when complexed to a carbocation). This model consists of pyrophosphate, two protons, one Mg^{2+} ion, and one formate. The Mg^{2+} ion bridges the two phosphate groups, as observed in X-ray structures of BPPS (Fig. 6c; similar arrangements are observed in many other terpene synthases).[17,18] This magnesium ion is also coordinated to both oxygen atoms of formate, a simple model of the aspartate group present in BPPS. In place of the other Mg^{2+} ions (and associated ligands) found in BPPS, we simply protonated one oxygen atom of each phosphate group and the hydrogen bonding pattern of the resulting hydroxyl groups was carefully chosen in each case to facilitate each reaction examined (alternative arrangements are described in the Supporting Information).‡[51]

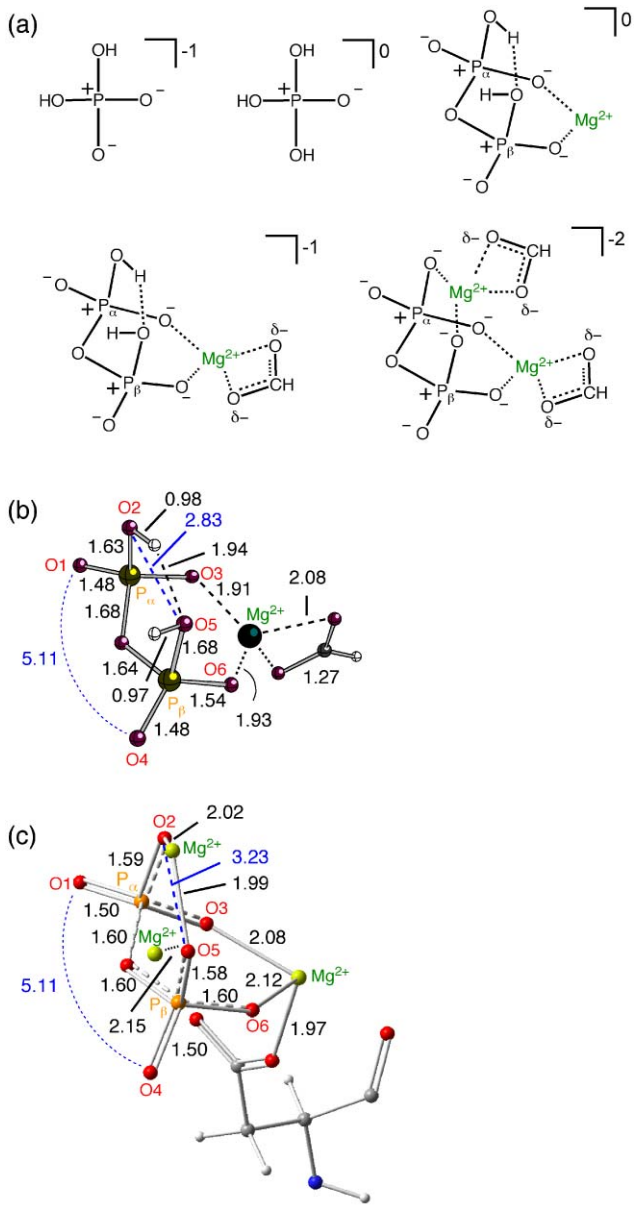

Fig. 6 (a) Five models of enzyme-bound pyrophosphate examined herein. (b) Computed geometry of the model (directly above) used in the remainder of our study (B3LYP/6-31G(d)). (c) Bound pyrophosphate from the crystal structure of BPPS (PDB id: 1N1Z).[18]

Using this model, we were able to locate two transition state structures, **TS3** and **TS4** (Fig. 7 and Scheme 5) that appeared to correspond to **TS1** and **TS2** (Fig. 4).[52] IRC calculations (Fig. 8a) verified that **TS3** connects the **B**-pyrophosphate complex to the BPP complex (**4**·Mg^{2+}–$HCOO^-$; Fig. 7 and Scheme 5). In the **B**-pyrophosphate complex, the diphosphate group interacts with **B** through both C4–H···O and C10–H···O interactions (Fig. 7). Note also that the C2–C7 bond distance is reduced to 1.64 Å upon complexation with the diphosphate group (compare with Fig. 1), leading to a more classical (although still hyperconjugated) structure. This geometric change makes sense in that the two C–H bonds that receive electron density from pyrophosphate oxygens are aligned with the formally empty p-orbital at C3 and therefore compete with the C2–C7 bond as hyperconjugative donors. The predicted energy barrier for BPP formation is approximately 10 kcal mol^{-1} from the **B**-pyrophosphate complex and this reaction is quite exothermic (Fig. 7). Note that the fully optimized geometry of the BPP complex deviates somewhat from the structure of BPP bound in the BPPS active site (primarily in terms of the position of the carboxylate attached to Mg and, to a lesser extent, the relative orientation of the bornyl and pyrophosphate groups; Fig. 9) as a result of the absence of the rest of the active site in our model; nonetheless, the key bonding features of the product complex are captured in our model.[18]

IRC calculations also indicate that **TS4** connects the **D**-pyrophosphate complex to the BPP complex (Scheme 5, Fig. 7 and 8b), in analogy to the reaction involving **TS2** (Fig. 4). However, although the pathways for BPP formation *via* **TS3** and **TS4** are related to each other, they do not appear to merge as did the analogous pathways using ammonia or water nucleophiles. Geometries along the IRC path from **TS3** differ subtly from those along the IRC path from **TS4** (Fig. 8a,b). Note that the β-phosphate group of the pyrophosphate interacts with a hydrogen at C2 as the pyrophosphate group attacks the pinyl cation, while different interactions of the β-phosphate group occur during attack of the pyrophosphate group on the camphyl cation (although this difference could, in principle, be overcome by the enforcement of particular conformations in the enzyme active site).

We predict that, if formed in BPPS, *either the camphyl or the pinyl cation can serve as a direct precursor of BPP* (Schemes 4 and 5). The viability of forming BPP directly from the camphyl cation is also supported by the QM/MM calculations of Weitman and Major, from which a free energy barrier of approximately 5 kcal mol^{-1} and an exergonicity of approximately 25 kcal mol^{-1} in the presence of the enzyme was estimated.[23] Note that calculations with our model system lead to an estimated barrier of 8–9 kcal mol^{-1} and an exothermicity of approximately 30 kcal mol^{-1} (Fig. 7; entropy corrections are not included in these estimates).

To date, however, we have been unable to find a transition state structure for the direct interconversion of the pinyl cation and the

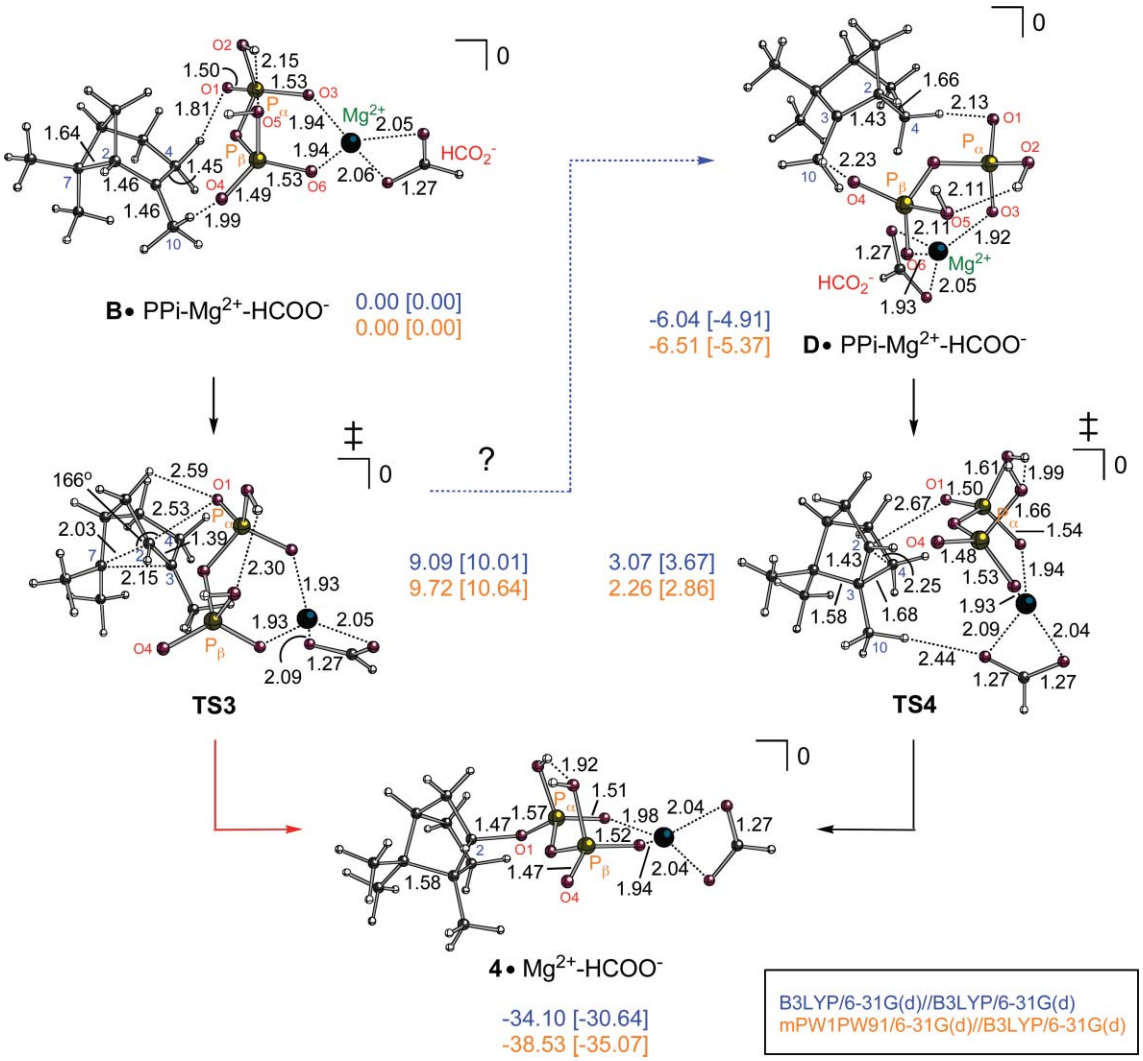

Fig. 7 Formation of bornyl diphosphate (BPP). Computed reactant complexes, transition state structures and product complex (selected distances in Å; energies in kcal mol^{-1}: before and after zero-point energy corrections from B3LYP frequency calculation in normal text and in brackets, respectively).

camphyl cation in the presence of pyrophosphate for the binding mode corresponding to the X-ray structure of bound BPP.[18,53] This appears to be the result of the nucleophilicity and position (Fig. 7) of the bound pyrophosphate group. As C7 moves from C2 to C3—the leading event in the **B**-to-**D** rearrangement—and positive charge accumulates on C2, the nearby pyrophosphate attacks C2, preventing **D** formation and leading directly to BPP. Thus, the **D**-to-BPP reaction, although energetically viable on its own,[23] may not be a major source of BPP from BPPS. We suggest that in order for this process to occur (in BPPS or other terpene synthases), a different cation-pyrophosphate binding mode must be involved in which the nucleophilic oxygens of the pyrophosphate group are kept away from C2 and the **B**-to-**D** rearrangement is allowed to proceed uninterrupted. Such a binding mode could be involved throughout the **A**-to-BPP process (although this seems more likely for enzymes that do not make BPP as their main product) or, perhaps, be adopted only transiently (what we refer to as a "dynamically controlled on/off" mechanism) if formation of **D** (and then the camphenes; *vide infra*) is desired.[54]

Formation of olefinic monoterpenes

There is no doubt that the nature of the base present in the active site of a given terpene synthase plays a key role in product distributions. Despite speculation surrounding the identities of active site bases in terpene synthase-mediated reactions, firm evidence for the identity of any active site base remains elusive.[4,18,55] From time to time, it has been suggested that bound pyrophosphate serves as the base.[5b] Calculations using our pyrophosphate model system suggest that this is indeed energetically viable. For example, models of deprotonation to yield α/β-pinene (Scheme 4) are shown in Fig. 10; deprotonation barriers for these cases are predicted to be low and the deprotonation processes are predicted to be exothermic.[56] If the orientation of bound pyrophosphate is similar to that in our model complexes, then mixtures of α- and β-pinene are expected, and to our knowledge, mixtures of α- and β-pinene are always produced by pinene-synthesizing enzymes (although their relative ratios vary).[1,15,19,57] Similar low-barrier deprotonation pathways to form α- and β-camphene (Scheme 4) from complexes

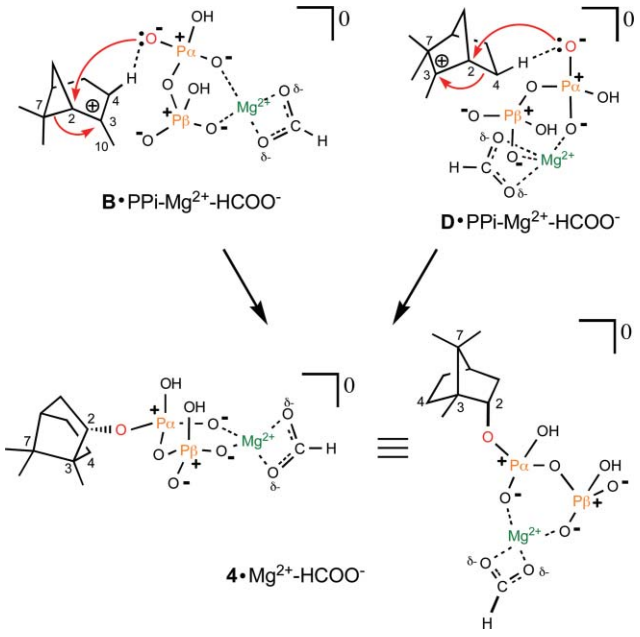

Scheme 5

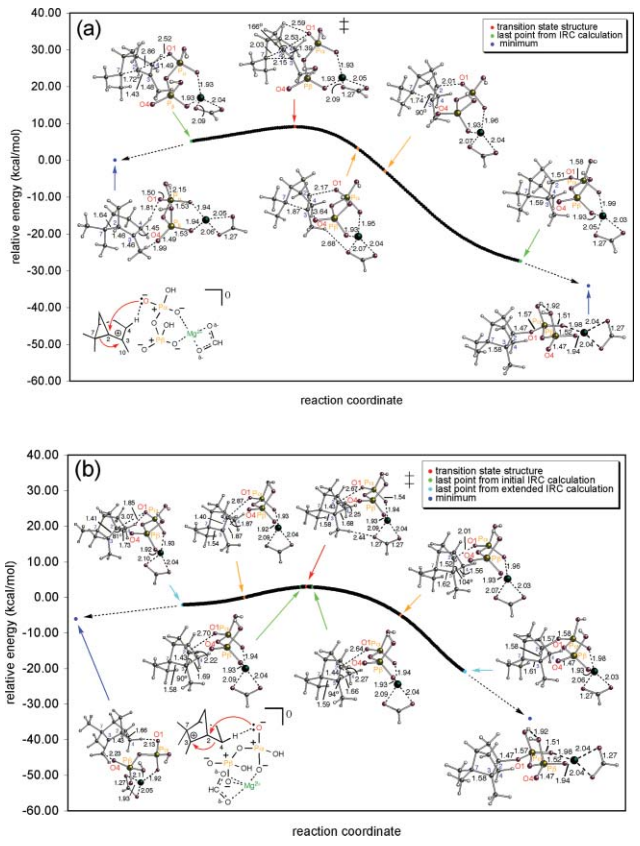

Fig. 8 Conversion of **B**-PPi-Mg^{2+}-$HCOO^-$ (a) and **D**-PPi-Mg^{2+}-$HCOO^-$ (b) to **4** complexed with Mg^{2+} and $HCOO^-$ from IRC calculations (B3LYP/6-31G(d)). For the IRC plot in (b), calculations in both directions were extended using the wavefunction, geometry and force constants from the last point of the previous IRC calculation (*i.e.*, using "rcfc").

of **D** were also found (see Supporting Information‡), although, as discussed above, active avoidance of BPP formation appears to be necessary to form these monoterpenes.[58]

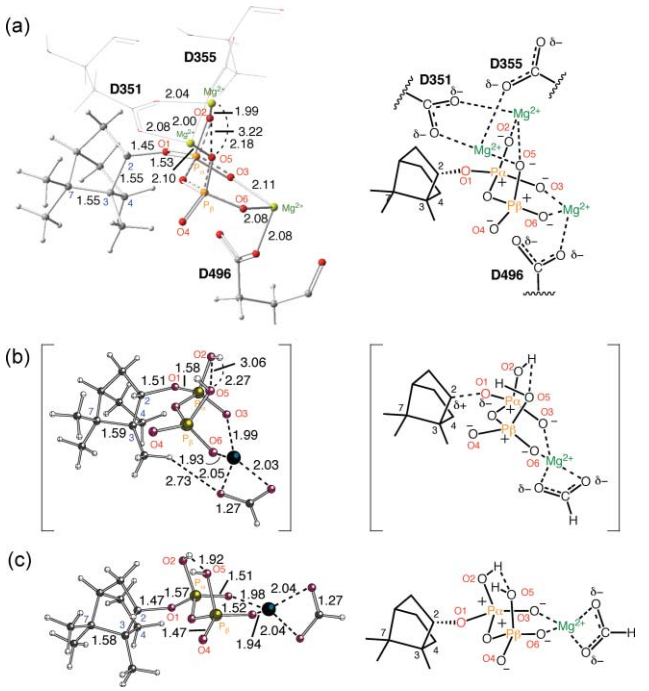

Fig. 9 (a) BPP complex in BPPS (atomic coordinates from the X-ray crystal structure of the BPPS-BPP complex (PDB id: 1N24)).[18] (b) The last point from the IRC calculation from **TS3** toward BPP (B3LYP/6-31G(d)). (c) Fully optimized BPP complex (B3LYP/6-31G(d)).

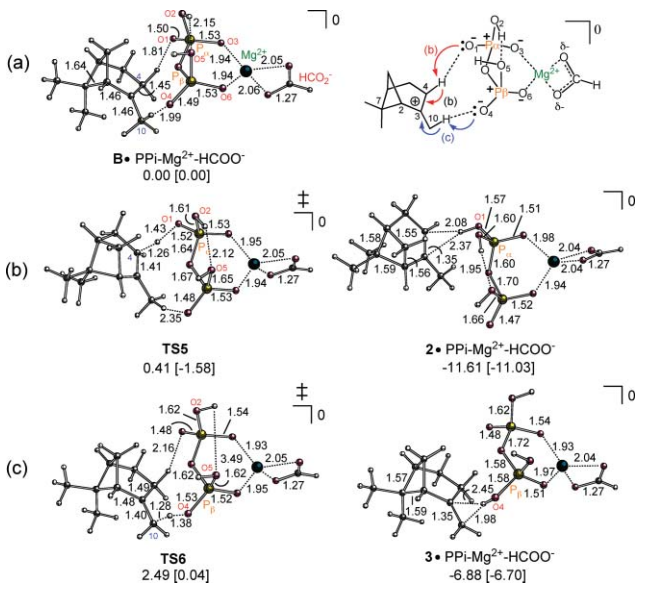

Fig. 10 Formation of α/β-pinene. Computed (B3LYP/6-31G(d)) geometries (selected distances in Å) and energies (in kcal mol^{-1}, and before and after zero-point energy corrections in normal text and in brackets, respectively) are shown. (a) **B**-PPi-Mg^{2+}-$HCOO^-$ complex and schematic picture of the two deprotonation pathways. (b) Transition state structure for deprotonation to form α-pinene and α-pinene complex with PPi-Mg^{2+}-$HCOO^-$. (c) Transition state structure for deprotonation to form β-pinene and β-pinene complex with PPi-Mg^{2+}-$HCOO^-$.

Conclusions

In the absence of an enzyme, we predict that the terpinyl cation can cyclize to the pinyl cation, which can then rearrange to the camphyl

cation *via* a concerted dyotropic reaction (double alkyl shift). The secondary bornyl cation, which was previously proposed to be a direct precursor to bornyl diphosphate, is instead predicted to occur along the reaction coordinate for the pinyl cation-to-camphyl cation rearrangement, in the region of the transition state structure. This result persists at a variety of different levels of theory. Based on our results using a new model of enzyme-bound pyrophosphate, we predict that either the pinyl cation or the camphyl cation can be a direct precursor to bornyl diphosphate. While both of these transformations are viable energetically, the most direct route[59] would involve attack of pyrophosphate on the pinyl cation. We suggest that this process is more likely than the camphyl cation route for the cation binding orientation expected for BPPS. Our quantum chemical calculations also provide support for the energetic viability of deprotonation by enzyme-bound pyrophosphate to produce alkene products.

Acknowledgements

We gratefully acknowledge UC Davis, the National Science Foundation, and the Pittsburgh Supercomputer Center for support and Michael Lodewyk for helpful comments.

References

1 Leading references: (*a*) M. Gijzen, E. Lewinsohn and R. Croteau, *Arch. Biochem. Biophys.*, 1992, **294**, 670–674; (*b*) C. Funk, E. Lewinsohn, B. S. Vogel, C. L. Steele and R. Croteau, *Plant Physiol.*, 1994, **106**, 999–1005; (*c*) E. Lewinsohn, M. Gijzen, R. M. Muzika, K. Barton and R. Croteau, *Plant Physiol.*, 1993, **101**, 1021–1028; (*d*) M. Gijzen, E. Lewinsohn and R. Croteau, *Arch. Biochem. Biophys.*, 1991, **289**, 267–73; (*e*) C. L. Steele, E. Lewinsohn and R. Croteau, *Proc. Natl. Acad. Sci. U. S. A.*, 1995, **92**, 4164–4168; (*f*) E. Lewinsohn, M. Gijzen, T. J. Savage and R. Croteau, *Plant Physiol.*, 1991, **96**, 38–43; (*g*) E. Lewinsohn, M. Gijzen and R. Croteau, *Plant Physiol.*, 1991, **96**, 44–49.
2 D. McCaskill and R. Croteau, *Adv. Biochem. Eng. Biotechnol.*, 1997, **55**, 107–146.
3 (*a*) E. M. Davis and R. Croteau, *Top. Curr. Chem.*, 2000, **209**, 53–95; (*b*) R. Croteau, *Chem. Rev.*, 1987, **87**, 929–954.
4 A. Roy, F. G. Roberts, P. R. Wilderman, K. Zhou, R. J. Peters and R. M. Coates, *J. Am. Chem. Soc.*, 2007, **129**, 12453–12460.
5 (*a*) B. T. Greenhagen, P. E. O'Maille, J. P. Noel and J. Chappell, *Proc. Natl. Acad. Sci. U. S. A.*, 2006, **103**, 9826–9831; (*b*) E. Y. Shishova, L. Di Costanzo, D. E. Cane and D. W. Christianson, *Biochemistry*, 2007, **46**, 1941–1951; (*c*) R. J. Peters and R. B. Croteau, *Arch. Biochem. Biophys.*, 2003, **417**, 203–211.
6 M. W. Lodewyk, P. G. Gutta and D. J. Tantillo, *J. Org. Chem.*, 2008, **73**, 6570–6579.
7 P. Gutta and D. J. Tantillo, *J. Am. Chem. Soc.*, 2006, **128**, 6172–6179.
8 S. C. Wang and D. J. Tantillo, *Org. Lett.*, 2008, **10**, 4827–4830.
9 Y. J. Hong and D. J. Tantillo, *Org. Biomol. Chem.*, 2009, **7**, 4101–4109.
10 Y. J. Hong and D. J. Tantillo, *J. Am. Chem. Soc.*, 2009, **131**, 7999–8015.
11 Y. J. Hong and D. J. Tantillo, *Org. Lett.*, 2006, **8**, 4601–4604.
12 P. Gutta and D. J. Tantillo, *Org. Lett.*, 2007, **9**, 1069–1071.
13 Y. J. Hong and D. J. Tantillo, *Nat. Chem.*, 2009, **1**, 384–389.
14 Y. J. Hong and D. J. Tantillo, *J. Am. Chem. Soc.*, 2010, **132**, 5375–5386.
15 (*a*) R. B. Croteau, C. J. Wheeler, D. E. Cane, R. Ebert and H. J. Ha, *Biochemistry*, 1987, **26**, 5383–5389; (*b*) K. C. Wagschal, H.-J. Pyun, R. M. Coates and R. Croteau, *Arch. Bioch. Biophys.*, 1994, **308**, 477–487; in this paper, however, it was concluded that, "the pinyl cation can, in fact, serve as a branch-point intermediate in the biosynthesis of both (–)-camphene and the (–)-pinene isomers," at least in some systems.
16 (*a*) R. Croteau, C. J. Wheeler, R. Aksela and A. C. Oehlschlager, *J. Biol. Chem.*, 1986, **261**, 7257–7263; (*b*) R. B. Croteau, J. J. Shaskus, B. Renstrom, N. M. Felton, D. E. Cane, A. Saito and C. Chang, *Biochemistry*, 1985, **24**, 7077–7085; (*c*) H. Gambliel and R. Croteau, *J. Biol. Chem.*, 1984, **259**, 740–748; (*d*) H. Gambliel and R. Croteau, *J. Biol. Chem.*, 1982, **257**, 2335–2342.
17 D. W. Christianson, *Chem. Rev.*, 2006, **106**, 3412–42.
18 D. A. Whittington, M. L. Wise, M. Urbansky, R. M. Coates, R. B. Croteau and D. W. Christianson, *Proc. Natl. Acad. Sci. U. S. A.*, 2002, **99**, 15375–15380.
19 (*a*) W. Schwab, D. C. Williams, E. M. Davis and R. Croteau, *Arch. Biochem. Biophys.*, 2001, **392**, 123–136; (*b*) M. L. Wise, T. J. Savage, E. Katahira and R. Croteau, *J. Biol. Chem.*, 1998, **273**, 14891–14899.
20 D. J. Tantillo, *Org. Lett.*, 2010, **12**, 1164–1167.
21 Y. J. Hong and D. J. Tantillo, *J. Org. Chem.*, 2007, **72**, 8877–8881.
22 M. D. Bojin and D. J. Tantillo, *J. Phys. Chem. A*, 2006, **110**, 4810–4816.
23 M. Weitman and D. T. Major, *J. Am. Chem. Soc.*, 2010, **132**, 6349–6360.
24 M. J. Frisch, G. W. Trucks, H. B. Schlegel, G. E. Scuseria, M. A. Robb, J. R. Cheeseman, J. A. Montgomery, Jr., T. Vreven, K. N. Kudin, J. C. Burant, J. M. Millam, S. S. Iyengar, J. Tomasi, V. Barone, B. Mennucci, M. Cossi, G. Scalmani, N. Rega, G. A. Petersson, H. Nakatsuji, M. Hada, M. Ehara, K. Toyota, R. Fukuda, J. Hasegawa, M. Ishida, T. Nakajima, Y. Honda, O. Kitao, H. Nakai, M. Klene, X. Li, J. E. Knox, H. P. Hratchian, J. B. Cross, V. Bakken, C. Adamo, J. Jaramillo, R. Gomperts, R. E. Stratmann, O. Yazyev, A. J. Austin, R. Cammi, C. Pomelli, J. Ochterski, P. Y. Ayala, K. Morokuma, G. A. Voth, P. Salvador, J. J. Dannenberg, V. G. Zakrzewski, S. Dapprich, A. D. Daniels, M. C. Strain, O. Farkas, D. K. Malick, A. D. Rabuck, K. Raghavachari, J. B. Foresman, J. V. Ortiz, Q. Cui, A. G. Baboul, S. Clifford, J. Cioslowski, B. B. Stefanov, G. Liu, A. Liashenko, P. Piskorz, I. Komaromi, R. L. Martin, D. J. Fox, T. Keith, M. A. Al-Laham, C. Y. Peng, A. Nanayakkara, M. Challacombe, P. M. W. Gill, B. G. Johnson, W. Chen, M. W. Wong, C. Gonzalez and J. A. Pople, *GAUSSIAN 03 (Revision D.01)*, Gaussian, Inc., Wallingford, CT, 2004.
25 (*a*) A. D. Becke, *J. Chem. Phys.*, 1993, **98**, 5648–5652; A. D. Becke, *J. Chem. Phys.*, 1993, **98**, 1372–1377; (*b*) C. Lee, W. Yang and R. G. Parr, *Phys. Rev. B: Condens. Matter*, 1988, **37**, 785–789; (*c*) P. J. Stephens, F. J. Devlin, C. F. Chabalowski and M. J. Frisch, *J. Phys. Chem.*, 1994, **98**, 11623–11627.
26 P. Gutta and D. J. Tantillo, *Angew. Chem., Int. Ed.*, 2005, **44**, 2719–2723.
27 G. A. Ho, D. H. Nouri and D. J. Tantillo, *J. Org. Chem.*, 2005, **70**, 5139–5143.
28 I. D. Mackie, J. Govindhakannan and G. A. DiLabio, *J. Phys. Chem. A*, 2008, **112**, 4004–4010.
29 S. P. T. Matsuda, W. K. Wilson and Q. Xiong, *Org. Biomol. Chem.*, 2006, **4**, 530–543.
30 C. Adamo and V. Barone, *J. Chem. Phys.*, 1998, **108**, 664–675.
31 J. P. Perdew, K. Burke and M. Ernzerhof, *Phys. Rev. Lett.*, 1996, **77**, 3865.
32 Y. Zhao and D. G. Truhlar, *J. Phys. Chem. A*, 2004, **108**, 6908–6918.
33 Y. Zhao, B. J. Lynch and D. G. Truhlar, *J. Phys. Chem. A*, 2004, **108**, 2715–2719.
34 (*a*) W. J. Hehre, L. Radom, P. v. R. Schleyer and J. A. Pople, *Ab Initio Molecular Orbital Theory*, John Wiley & Sons, New York, 1986; (*b*) C. Møller and M. S. Plesset, *Phys. Rev.*, 1934, **46**, 618–622.
35 (*a*) C. Gonzalez and H. B. Schlegel, *J. Phys. Chem.*, 1990, **94**, 5523–5527; (*b*) K. Fukui, *Acc. Chem. Res.*, 1981, **14**, 363–368.
36 N. Müller, A. Falk and G. Gsaller, *Ball & Stick V.4.0a12, molecular graphics application for MacOS computers*, Johannes Kepler University, Linz, 2004.
37 Similarly long "bonds" have been found in other terpene-related cases[6,7,38].
38 D. J. Tantillo, *Chem. Soc. Rev.*, 2010, **39**, 2847–2854.
39 (*a*) C. Jenson and W. L. Jorgensen, *J. Am. Chem. Soc.*, 1997, **119**, 10846–10854; (*b*) P. C. Miklis, R. Ditchfield and T. A. Spencer, *J. Am. Chem. Soc.*, 1998, **120**, 10482–10489; (*c*) F. Antonello, R. Graziella, R. Gabriele, G. Felice and S. Maurizio, *Chem.– Eur. J.*, 2003, **9**, 2072–2078; (*d*) H. Dietmar, *Angew. Chem., Int. Ed.*, 2002, **41**, 3208–3210.
40 (*a*) I. V. Vrcek, V. Vrcek and H.-U. Siehl, *J. Phys. Chem. A*, 2002, **106**, 1604–1611; (*b*) D. Farcasiu, P. Lukinskas and S. V. Pamidighantam, *J. Phys. Chem. A*, 2002, **106**, 11672–11675; (*c*) M. R. Siebert and D. J. Tantillo, *J. Org. Chem.*, 2006, **71**, 645–654.
41 See Supporting Information for details‡. We have exploited ammonia to assess structural distortions of carbocations previously[6,10,14,21,22,26].
42 D. J. Tantillo, *J. Phys. Org. Chem.*, 2008, **21**, 561–570.
43 (*a*) D. H. Nouri and D. J. Tantillo, *J. Org. Chem.*, 2006, **71**, 3686–3695; (*b*) M. T. Reetz, *Angew. Chem., Int. Ed. Engl.*, 1972, **11**, 130–131; (*c*) M. T. Reetz, *Angew. Chem., Int. Ed. Engl.*, 1972, **11**, 129–130; (*d*) M. T. Reetz, *Tetrahedron*, 1973, **29**, 2189–2194; (*e*) M. T. Reetz, *Adv. Organomet. Chem.*, 1977, **16**, 33–65; (*f*) I. Fernandez, F. P. Cossio and

M. A. Sierra, *Chem. Rev.*, 2009, **109**, 6687–6711; (*g*) R. L. Davis and D. J. Tantillo, *J. Org. Chem.*, 2010, **75**, 1693–1700.
44 (*a*) J. B. A. Hess, *J. Am. Chem. Soc.*, 2002, **124**, 10286–10287; (*b*) J. B. A. Hess and L. Smentek, *Org. Lett.*, 2004, **6**, 1717–1720; (*c*) J. B. A. Hess, *Org. Lett.*, 2003, **5**, 165–167.
45 Pinene and camphene are also related to the sesquiterpenes bergamotene and santalene, respectively. See: (*a*) C. G. Jones, E. L. Ghisalberti, J. A. Plummer and E. L. Barbour, *Phytochemistry*, 2006, **67**, 2463–2468; (*b*) C. Schnee, T. G. Köllner, M. Held, T. C. Turlings, J. Gershenzon and J. Degenhardt, *Proc. Natl. Acad. Sci. U. S. A.*, 2006, **103**, 1129–1134; (*c*) T. G. Köllner, C. Schnee, J. Gershenzon and J. Degenhardt, *Plant Cell*, 2004, **16**, 1115–1131; (*d*) S. Gallori, A. R. Bilia, N. Mulinacci, C. Bicchi, P. Rubiolo and F. F. Vincieri, *Planta Med.*, 2001, **67**, 290–292; (*e*) A. T. Kreipl and W. A. Konig, *Phytochemistry*, 2004, **65**, 2045–2049; (*f*) We will describe calculations on these systems in due course.
46 In some cases, this may be a result of post-transition state bifurcations[13,23,43a,47].
47 D. H. Ess, S. E. Wheeler, R. R. lafe, L. Xu, N. Celebi-Ölcüm and K. N. Houk, *Angew. Chem., Int. Ed.*, 2008, **47**, 7592–7601.
48 The camphyl cation was also studied in detail by Sorensen and co-workers using B3LYP, MP2, MP3(full), MP4(SDQ) and QCI calculations; see: P. Brunelle, T. S. Sorensen and C. Taeschler, *J. Org. Chem.*, 2001, **66**, 7294–7302.
49 Note that the C4–$H_{exo}\cdots$N interaction is favorable for deprotonation to form α-pinene and the C10–H$\cdots$N interaction is favorable for deprotonation to form β-pinene. Computations on these deprotonation reactions are described in the Supporting Information‡.
50 We also examined attack of ammonia on C2 from the lefthand side of **D** to form the C2 epimer of **7**-H^+. This reaction also involves concerted alkyl shift/ammonia addition and has a barrier of approximately 8 kcal mol^{-1}. See Supporting Information‡ for details.
51 There is also a water in the active site of BPPS, but it is on the side of the hydrocarbon framework opposite to the pyrophosphate, approximately 3.8 Å away from C2 (see Supporting Information for pictures‡)[18].
52 The B3LYP/6-31G(d) method was used for all of the pyrophosphate complexes due to their size. Test calculations using B3LYP/6-31+G(d,p) gave similar results. Details can be found in the Supporting Information‡. We also performed single point energy calculations using the BB1K, mPWB1K and MP2 methods on the B3LYP geometries shown in Fig. 7. The results led to similar conclusions as those based on the B3LYP/6-31G(d) calculations; see Supporting Information for these energies‡.
53 Our attempts included the use of constrained calculations and even larger models involving 3 magnesium ions; invariably, however, C–O bond formation occurred. We did find transition state structures for the direct interconversions of the pinyl cation and the camphyl cation in the presence of ammonia; see Supporting Information for details‡.
54 (*a*) A recent study on mechanism-based inhibition of pinene synthase suggested that intermolecular contacts between intermediates and the enzyme change during the course of rearrangement reactions. See: P. McGeady and R. Croteau, *Arch. Biochem. Biophys.*, 1995, **317**, 149–155. In addition, it appears that significant space may exist in the BPPS active site,[18] perhaps allowing cation **B**, which is much more compact than GPP, to rotate, at least slightly; (*b*) We did find a pathway for the interconversion of bound **B** and **D**, but this involved a considerably different binding mode and a transition state structure that was approximately 10 kcal mol^{-1} higher in energy than **TS3** (Fig. 7). This pathway is quite complicated, however. The transition state structure in question actually appears to be connected on one side directly to a camphene (*i.e.*, deprotonated **D**) complex and on the other side to another transition state structure that connects complexes of **A** and **B** (*i.e.*, the pathway down from the transition state structure appears to bifurcate). See Supporting Information for details.‡ Moreover, this reaction scheme appears to be consistent with previously reported kinetic isotope effect data for pinene synthase,[15] although the dynamics of moving along such pathways are likely to be complicated.
55 (*a*) C. A. Lesburg, G. Zhai, D. E. Cane and D. W. Christianson, *Science*, 1997, **277**, 1820–1824; (*b*) M. Xu, P. R. Wilderman and R. J. Peters, *Proc. Natl. Acad. Sci. U. S. A.*, 2007, **104**, 7397–7401.
56 Simple deprotonation models using ammonia as a base can be also found in the Supporting Information‡.
57 (*a*) S. Lu, R. Xu, J. W. Jia, J. Pang, S. P. Matsuda and X. Y. Chen, *Plant Physiol.*, 2002, **130**, 477–486; (*b*) M. A. Phillips, M. R. Wildung, D. C. Williams, D. C. Hyatt and R. Croteau, *Arch. Biochem. Biophys.*, 2003, **411**, 267–276; (*c*) K. C. Wagschal, H. J. Pyun, R. M. Coates and R. Croteau, *Arch. Biochem. Biophys.*, 1994, **308**, 477–487; (*d*) R. Croteau and D. M. Satterwhite, *J. Biol. Chem.*, 1989, **264**, 15309–15315; (*e*) K. P. Adam and R. Croteau, *Phytochemistry*, 1998, **49**, 475–480; (*f*) J. Bohlmann, C. L. Steele and R. Croteau, *J. Biol. Chem.*, 1997, **272**, 21784–21792.
58 Formation of limonene was also examined; see Supporting Information for details‡.
59 R. Hoffmann, V. I. Minkin and B. K. Carpenter, *HYLE-Int. J. Phil. Chem.*, 1997, **3**, 3–28 (reprinted from: *Bull. Soc. Chim. Fr.*, 1996, **133**, 117–130).

